

# Rheological properties and fiber orientations of short fiber-reinforced plastics

Jin Kon Kim<sup>a)</sup> and Ju Ho Song

*Department of Chemical Engineering, Pohang University of Science and Technology, Pohang, Kyungbuk 790-784, Korea*

(Received 3 February 1997; final revision received 2 May 1997)

## Synopsis

The effect of fiber orientation on the rheological properties of short glass fiber-reinforced composites was investigated by dynamic oscillatory shearing with parallel plate fixtures. As an oscillatory shear amplitude and frequency applied to fiber-reinforced composites increased, more fibers in the composites were aligned in the flow direction, thus the complex viscosity gradually decreased. This phenomenon was confirmed by observing the fiber orientations using optical photographs. The complex viscosity depended upon the strain amplitude, and pre-oscillatory shearing frequency, and shearing time. Experimental results for fiber orientations and complex viscosity were compared with predictions available at the present time. The predictions of the dependence of fiber orientation upon strain amplitudes and fiber volume fractions are in qualitative agreement with experimental data. However, there were effects of the magnitude of frequency and oscillatory shearing time on fiber orientation, thus complex viscosity could not be predicted successfully although these effects were clearly demonstrated by the experiment. © 1997 The Society of Rheology. [S0148-6055(97)00805-5]

## I. INTRODUCTION

Short glass fiber-reinforced composites are a class of engineering materials of growing commercial importance. These composites possess improved stiffness, strength, and heat distortion temperature in comparison with base polymers. Although mechanical properties of short-fiber composites are not as good as composites with long continuous reinforcing fibers, they have been widely used in industry due to better processability and lower processing cost. Mechanical properties of a part made of a short fiber composite are strongly dependent on the way the part is manufactured. This is because the orientation of fibers changes during material processing from molten states to the solidification of the matrix. Owing to the anisotropic property of a composite, maximum reinforcement can be obtained only when fibers are properly oriented [Tucker and Advani (1994)]. Therefore, it is very important to have some insight into the change of fiber orientation during flow, and to find some relationship between fiber orientations and macroscopically observable rheological properties such as viscosity and elasticity.

Rheological properties of particle (or glass fiber) reinforced polymers have been studied for a long time [Ausias *et al.* (1992); Becraft and Metzger (1992); Creasy *et al.* (1996); Czarnecki and White (1980); Greene and Wilkes (1995); Kobayashi *et al.* (1995); Laun (1984); Lobe and White (1979); Tanaka and White (1980); Wang and Inn (1994)],

---

<sup>a)</sup>Corresponding author; Electronic mail: jkkim@ced.postech.ac.kr

**TABLE I.** The molecular characteristics of polymers employed in this study.

Polymer	Molecular weight	Polydispersity	Trade name and Supplier
PS	$M_w^a = 322\,000$	2.3	GPPS-G116 (Dongbu Petrochemical Co., Korea)
PBT	$M_v^b = 44\,000$	2.2	Lupox GP-1000 (LG Chemicals Co., Korea)

<sup>a</sup>Weight-average molecular weight.<sup>b</sup>Viscosity-average molecular weight.

and they depend very sensitively on particle size, shape, content, and surface condition. [Han (1981); Tucker and Advani (1994); White (1990)]. Laun (1984) reported that a change of fiber orientation during shear flow gives rise to a pronounced overshoot of shear stress and of normal stress before reaching a steady value. However, it is rather difficult to find a theory(s) to explain this phenomenon because of the difficulty in estimating the effect of fiber orientation on rheological properties.

Recently, Greene and Wilkes (1995) studied the rheological properties of short fiber-reinforced thermoplastics using steady and dynamic shear measurement and showed that at lower shear rates ( $\dot{\gamma}$ ) the steady shear viscosity [ $\eta(\dot{\gamma})$ ] of fiber-reinforced thermoplastics increases with the amount of fibers, while at higher  $\dot{\gamma}$  this becomes almost the same as  $\eta(\dot{\gamma})$  of the neat resin regardless of glass fiber content. This is attributed to the fact that at higher  $\dot{\gamma}$  fibers contribute very little, if any, to the viscoelastic properties of a composite due to short times available. Also, they observed that complex viscosity [ $\eta^*(\omega)$ ], and storage and loss moduli [ $G'(\omega)$  and  $G''(\omega)$ ] increase with the amount of the fibers only at lower frequencies ( $\omega$ ).

Many research groups [Advani and Tucker (1987), (1990); Batchelor (1971); Dinh and Armstrong (1984); Folgar and Tucker (1984); Hand (1962); Hinch and Leal (1973); Lipscomb *et al.* (1988); Ranganathan and Advani (1991), (1993); Shaqfeh and Fredrickson (1990)] have developed theoretical models which enabled them to relate quantitatively between processing conditions and fiber orientation since Jeffery (1922) solved analytically the motion of a single ellipsoidal particle immersed in a viscous fluid. Hand (1962) proposed a theory relating the stress tensor to the rate of deformation tensor for anisotropic fluids. These results were further incorporated into constitutive equations developed by Hinch and Leal (1973) and by Lipscomb *et al.* (1988). Batchelor (1971) used a slender body theory to calculate the stress in a suspension with aligned fibers when subjected to elongation along the fiber axis. Dinh and Armstrong (1984) applied Batchelor's theory to arbitrary flows and fiber orientation states. Folgar and Tucker (1984), Advani and Tucker (1987), (1990), and Ranganathan and Advani (1991), (1993) developed models for the orientation behavior of fibers in concentrated suspensions by adding a rotary diffusion term to Jeffery's equation in order to account for fiber-fiber interactions. Using a slender body theory, Shaqfeh and Fredrickson (1990) obtained the expression of the viscosity for suspensions both with full alignment to the flow direction and with random orientation.

In this study, we investigate the effect of fiber orientation on the rheological properties of short glass fiber-reinforced plastics by oscillatory shearing measurement. When an oscillatory shearing is applied to glass fiber-reinforced composites, the fiber orientations change and eventually reach the steady values after longer times of shearing. The rheological properties change according to fiber orientation. Fiber orientations during oscillatory shearing flow were observed by optical microscope (OM). Finally, these experi-

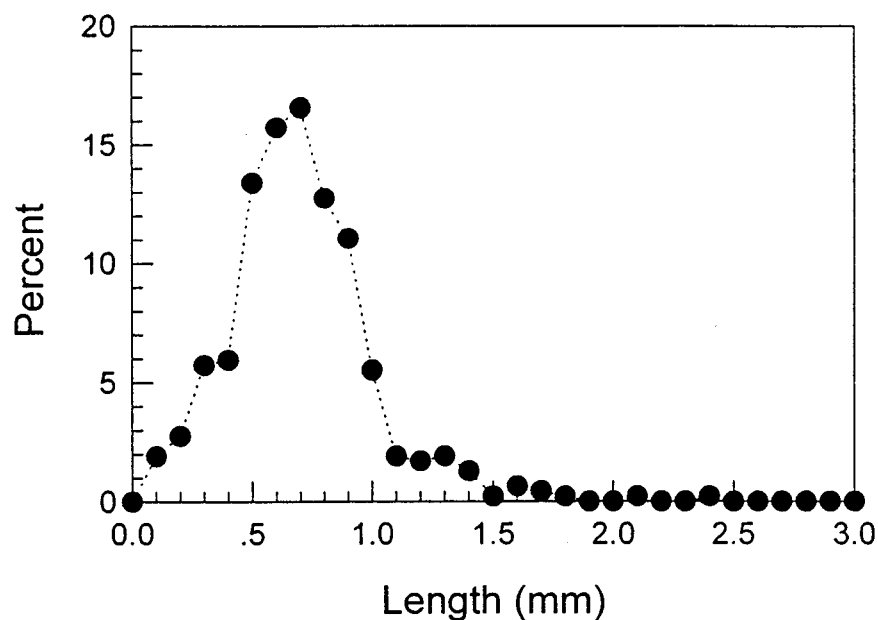


FIG. 1. Fiber length distribution of glass fibers in 80/20 (wt/wt) PS/glass fiber composite.

mental results were compared with predictions available at the present time [Advani and Tucker (1987), (1990); Ausias *et al.* (1992); Dinh and Armstrong (1984); Shaqfeh and Fredrickson (1990)].

## II. EXPERIMENT

### A. Material

The neat polymers employed in this study were commercial grades of polystyrene (PS) and poly(butylene terephthalate) (PBT), and their molecular characteristics are given in Table I. The glass fiber employed was a commercial product of Lucky-Dow Corning Co., Korea, with a length of 3 mm and a diameter of 13  $\mu\text{m}$ .

The glass fiber reinforced PS and PBT with various amounts (2–30 wt %) of glass fiber were prepared using an intermeshing corotating twin screw extruder (Tek Twin Extruder, Hankook Motronics Co., Korea;  $L/D = 28$ ,  $D = 30$  mm) at 220 and 250  $^{\circ}\text{C}$ , respectively, and pelletized by a rotary cutter. Before extrusion, PS and PBT polymers were dried at 110–120  $^{\circ}\text{C}$  for  $\sim 5$  h to remove any moisture. Each pellet was a cylindrical shape of 1 mm (diameter)  $\times$  3 mm (length), which was compression-molded for measurement of rheological properties. The fiber length in the composite was obtained using a hand-held caliper from OM photographs with the magnification of  $\times 50$  after the base polymer was completely burned out at 550  $^{\circ}\text{C}$  for 2 h. The fiber length distribution of glass fibers in 80/20 (wt/wt) PS/glass fiber composite is given in Fig. 1, from which the average fiber length is 0.7 mm with the standard deviation of 0.3 mm. The significant decrease in the fiber length from the original value (3 mm) is due to the breakage of glass fibers during the melt blending with neat PS in a twin-screw extruder even though the glass fibers were fed into the second hopper in the extruder to minimize fiber breakage.

It is noted that further breakage of glass fibers *does not* occur during the compression molding process or rheological measurement.

The glass fiber reinforced poly(propylene) (filled PP) was a commercial product, Topolene 5203G6 with 30 wt % of glass fiber and 10 wt % of mica, of Tongyang Nylon Co., Korea. The neat polypropylene employed in filled PP was a homopolymer type for an injection molding purpose (Trade name: J700; Tongyang Nylon Co., Korea) and its melt index (MI) based on ASTM D 1238 was 11 g/10 min. The weight average molecular weight ( $M_W$ ) was calculated to be  $2.5 \times 10^5$  from an empirical relationship of  $\log M_W = 5.674 - 0.272 \log (\text{MI})$  supplied by the producer. Finally, calcium carbonate ( $\text{CaCO}_3$ ) reinforced polystyrene with 20 wt % of  $\text{CaCO}_3$  powder, having a spherical shape with a diameter of 1.8  $\mu\text{m}$ , was prepared by the same twin screw extruder employed in making glass fiber reinforced polystyrene in order to study the effect of the filler shape on the rheological properties.

## B. Rheological measurement

An RDS-II (Rheometrics Inc.) using the dynamic oscillatory mode with a parallel plates fixture (25 mm diameter) was used to measure complex viscosity [ $\eta^*(\omega)$ ], storage [ $G'(\omega)$ ], and loss modulus [ $G''(\omega)$ ] as functions of frequency ( $\omega$ ) of neat polymers and glass fiber-reinforced composites at various temperatures. Each frequency sweep at a given temperature was done within  $\sim 10$  min by increasing frequency from 0.1 to 100 rad/s. Then, the frequency was decreased from 100 to 0.1 rad/s within 1 min and a subsequent frequency sweep test was performed. Even if the time interval between frequency sweeps was increased to 10 min, the rheological properties do not change. Thus, we consider that the fibers in the filled polymer do not relax during this time interval. The strain amplitude was 0.15 otherwise specified.

The sample thickness inside the RDS-II was  $\sim 2$  mm. We chose the parallel plate fixture since the gap used in a cone and plate fixture is just 50  $\mu\text{m}$ , which is too short to eliminate the boundary effect of a rheometer on the fibers. According to Milliken and Powell (1994), the gap in a rheometer must be three times larger than the fiber length. Because the average length of short glass fibers employed in this study was 0.7 mm as shown in Fig. 1, a gap of  $\sim 2$  mm may reduce considerably the boundary effect, although we cannot exclude this effect completely due to the existence of some glass fibers with a length larger than 1 mm.

Because of using parallel plates, the shear rate at each position in the sample is not the same, but changes with radial position. All measurements were done under a nitrogen environment to reduce any possible degradation occurring at higher temperatures.

## C. Morphological measurement

After the rheological properties of the glass fiber reinforced PS were measured at each temperature, the fiber orientations at three different radial positions, namely  $r = 0, 5,$  and 10 mm, where  $r$  is the radial distance from the center of the sample, were observed by optical microscope (Zeiss Co.) with a magnitude of  $\times 50$ . After very careful cooling of the specimen in a rheometer from the molten state to a temperature lower than the glass transition of neat polymer by nitrogen for 1 min while maintaining almost the same gap size, we successfully removed the sample from the rheometer without changing its thickness and shape. It should be mentioned, however, that during the cooling process the torque in the rheometer must be carefully monitored in order to avoid any damage to the torque transducer.

We assumed that any change in fiber orientations during the cooling process can be minimized because of short cooling time. Thus, the fiber orientations in a sample observed by optical microscopy represent essentially the same as those in the sample during rheological measurement.

### III. RESULTS AND DISCUSSION

#### A. Rheological properties

Figure 2 gives changes in complex viscosity [ $\eta^*(\omega)$ ] with repeated frequency sweeps for the glass fiber reinforced PS (filled PS) with 20 wt % of glass fiber. It can be seen in Fig. 2 that at lower frequency ( $\omega$ ),  $\eta^*(\omega)$  measured during the second frequency sweep is lower than that measured during the first frequency sweep, but this approaches a constant value as further frequency sweeps are made. This can be explained by the fact that initial fiber orientations in filled PS prepared by compression molding changed steadily with applied frequencies. Since viscosity of a glass fiber reinforced polymer with glass fibers oriented parallel along the flow direction is lower than that with glass fibers oriented randomly, more glass fibers in the PS matrix can be oriented parallel along the flow direction as the frequency sweep test is continued.

Another interesting result seen in Fig. 2 is that the decrease in  $\eta^*(\omega)$  with repeated frequency sweeps is more evident as the measuring temperature is increased and  $\omega$  is decreased. For example, at  $\omega = 0.1$  rad/s, the ratio of  $\eta^*(\omega)$  taken during the first frequency sweep to that taken during the fifth frequency sweep increased from 1.25 at 180 °C to 3.42 at 240 °C. The results can be explained by the facts that

- (i) as the measuring temperature increases, and frequency decreases, glass fibers in a sample have more of a chance of being oriented along the flow direction due to lower matrix viscosity and much more available time for glass fibers to be oriented during measurement; and
- (ii) as the temperature decreases, the stress to align fibers along the flow direction increases, thus the fibers are oriented along the flow direction within very short times.

In other words, many fibers in a sample were already oriented along the flow direction even for rheological measurement at one or two frequencies, which results in no further decrease in  $\eta^*(\omega)$  with repeated frequency sweeps. The small change in  $\eta^*(\omega)$  at higher  $\omega$  with repeated frequency sweeps is attributed to the fact that the contribution of glass fibers in a sample to  $\eta^*(\omega)$  becomes less important due to shorter times available.

Although we do not present the change in  $\eta^*(\omega)$  with repeated frequency sweeps for neat PS, we found that  $\eta^*(\omega)$  had the same values regardless of frequency sweeps. Neat PS employed in this study was prepared by extruding as-received PS pellets using the same twin-screw extruder under the same processing conditions as those used to prepare filled PS. Based on Fig. 2 and the results for neat PS, we found that regardless of measuring temperatures,  $\eta^*(\omega)$  at  $\omega = 0.1$  rad/s measured during the fifth frequency sweep for filled PS was 1.5–1.8 times that for neat PS at specific temperatures. This suggests that when fiber orientations reach a steady state, temperature dependence of  $\eta^*(\omega)$  of the filled PS is almost the same as that for neat PS.

Figure 3 gives plots of  $\eta^*(\omega)$  vs  $G''(\omega)$  at 220 °C for filled PS with various fiber contents. These plots are very similar to plots of steady shear viscosity,  $\eta(\dot{\gamma})$  versus shear stress  $\tau_W$ , advocated by many research groups [Han (1981); White (1990)]. It can be seen that as fiber contents increase, the yield behavior can be clearly observed at lower

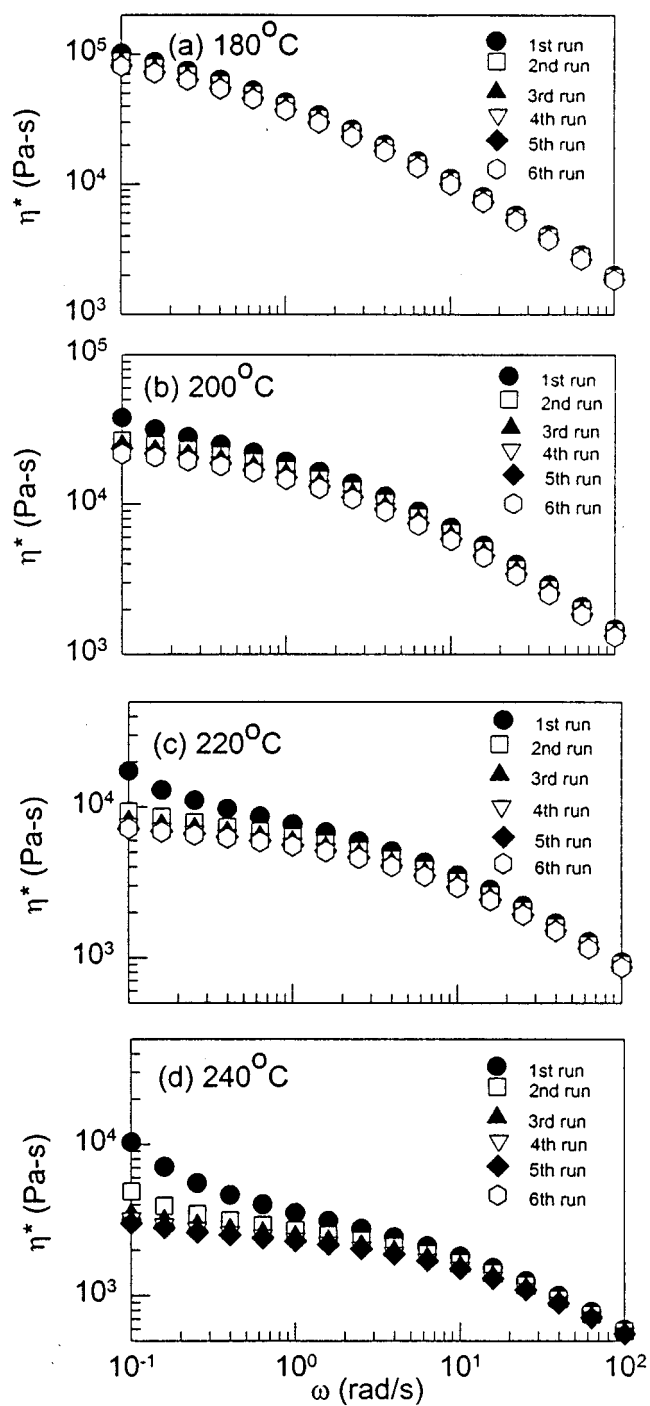


**FIG. 2.** Changes in complex viscosity ( $\eta^*$ ) with repeated frequency sweeps for 80/20 (wt/wt) PS/glass fiber at four different temperatures: (a) 180 °C, (b) 200 °C, (c) 220 °C, (d) 240 °C.

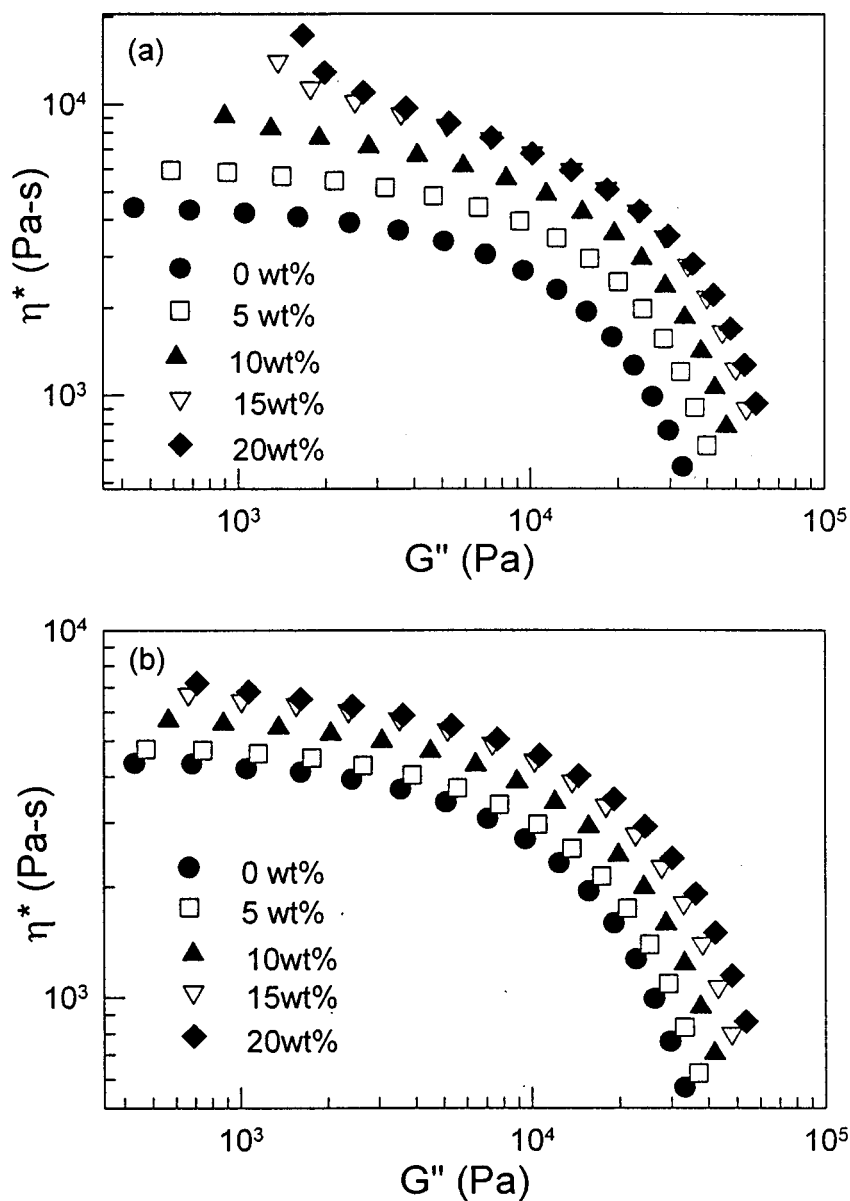
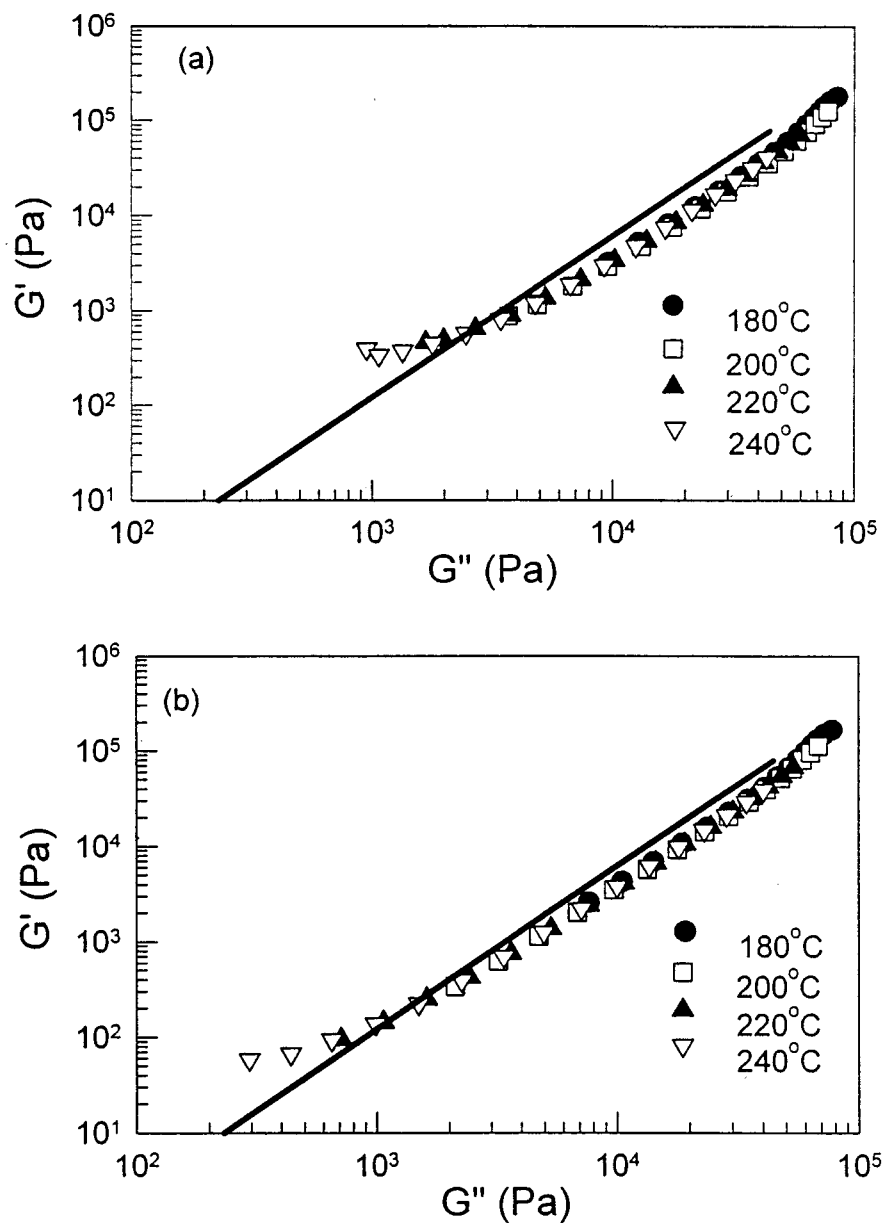


FIG. 3. Plots of  $\eta^*$  vs loss modulus ( $G''$ ) at 220 °C for filled PS with various fiber contents taken (a) during the first frequency sweep and (b) during the fifth frequency sweep.

$G''(\omega)$  when taken during the first frequency sweep. However, this yield behavior is barely seen even for filled PS with 20 wt % of fiber when taken during the fifth frequency sweep.

Log  $G'(\omega)$  vs log  $G''(\omega)$  plots for filled PS taken during the first frequency sweep and taken during the fifth frequency sweep are given in Figs. 4(a) and 4(b), respectively. Also, these plots for neat PS are shown as the solid line in Figs. 4(a) and 4(b). These plots are very sensitive to morphological change for polymer blends, block copolymers, and



**FIG. 4.** Log  $G'(\omega)$  vs log  $G''(\omega)$  plots of 80/20 (wt/wt) PS/glass fiber taken (a) during the first frequency sweep and (b) during the fifth frequency sweep at various temperatures ( $^{\circ}\text{C}$ ): (●) 180; (□) 200; (▲) 220, and (▽) 240. This plots for neat PS at four different temperatures are also given by the solid line in parts (a) and (b).

liquid crystal polymers, and exhibit temperature independence when morphology does not change with measuring temperatures [Han and Kim (1993)].

It can be seen in Fig. 4 that:

- (i) these plots for neat PS do not show temperature dependence (although data based

on four different temperatures is not shown in this figure to avoid overlapping) and the slope is about 1.8, which is due to polydispersity [Han and Kim (1989), (1993)];

- (ii) these plots for filled PS taken both during the first and during the fifth frequency sweeps *do not* show temperature dependence; and
- (iii) for smaller  $G''(\omega)$  (say  $\leq 10^3$  Pa),  $G'(\omega)$  at a given  $G''(\omega)$  taken during the first frequency sweep is larger than that taken during the fifth frequency sweep, whereas for larger  $G''(\omega)$ ,  $G'(\omega)$  at a given  $G''(\omega)$  taken during different frequency sweeps is almost the same.

It is rather interesting to find in Fig. 4 that although the values of  $G'(\omega)$  at lower  $G''(\omega)$  for filled PS are larger than those for neat PS, these values at higher  $G''(\omega)$  for filled PS are slightly *smaller* than those for neat PS. Previously, Czarnecki and White (1980) reported that the first normal stress,  $N_1$ , at given  $\tau_W$  for the glass fiber-reinforced PS is always larger than that for neat PS. The reason for this discrepancy is not clear although our study is based on the oscillatory shear experiment, while Czarnecki and White (1980) employed the steady shear experiment. We also found similar phenomena in the results of Czarnecki and White (1980) when a steady shear measurement was made for filled PS. However, for the filled PS employed in this study, the steady shear measurement was possible only until the total strain (shear rate times time;  $\dot{\gamma}t$ ) was up to about 20, whereas  $N_1$  at larger  $\dot{\gamma}$  (say,  $\dot{\gamma} \geq 5 \text{ s}^{-1}$ ) can still change until this time. We also found that the original cylindrical shape of a sample in the parallel plate fixture continuously changed to an oblate shape during steady shearing at longer times ( $\dot{\gamma}t > 20$ ). This suggests that the measured value of  $\tau_W$  and  $N_1$  may not be very accurate; thus we do not present the steady experimental data here.

We observed that even for filled PS with different amounts of the glass fiber (5, 10, and 15 wt % of glass fiber in a composite),  $\eta^*(\omega)$  decreased with repeated frequency sweeps which is very similar to the results given in Fig. 2, although the decrease in  $\eta^*(\omega)$  is less evident with decreasing glass fiber contents. It was also found that for filled PS with 20 wt % of  $\text{CaCO}_3$  powder having a spherical shape with a diameter of 1.8  $\mu\text{m}$ ,  $\eta^*(\omega)$  does not decrease with repeated frequency sweeps. This is attributed to the fact that an oscillatory shearing flow cannot change the orientation of  $\text{CaCO}_3$  due to the spherical powders having a size much less than the gap in a rheometer. By investigating stress-induced interfacial failure in glass bead-filled polymer melts, Wang and Inn (1994) showed that the decay of  $\eta^*(\omega)$  with oscillatory shearing time is caused by interfacial slippage due to high local stresses and this decayed  $\eta^*(\omega)$  can be recovered by the healing of fractured filler and polymer interfaces. However, the recovery of  $\eta^*(\omega)$  for the PS/fiber system employed in this study was never observed and this will be corroborated later. Therefore, we consider that the interfacial failure does not occur in this sample.

The decrease in  $\eta^*(\omega)$  with repeated frequency sweeps was also observed for two other filled polymer systems, one for PBT with 30 wt % glass fibers, and the other for PP with 30 wt % glass fibers and 10 wt % mica, shown in Figs. 5(a) and 5(b), respectively. It is noted that for neat PBT and PP polymers, we found that  $\eta^*(\omega)$  has the same value regardless of repeated frequency sweeps.

It can be concluded from Figs. 2 and 5 that rheological properties such as  $\eta^*(\omega)$ ,  $G'(\omega)$ , and  $G''(\omega)$ , for glass fiber-reinforced polymers can change with repeat measurements due to glass fiber orientations during oscillatory shearing, but these properties for neat polymer and filled polymer with spherical powders having a size much less than the gap in a rheometer do not change with repeat measurements as long as spheres are very small compared with a rheometer gap.

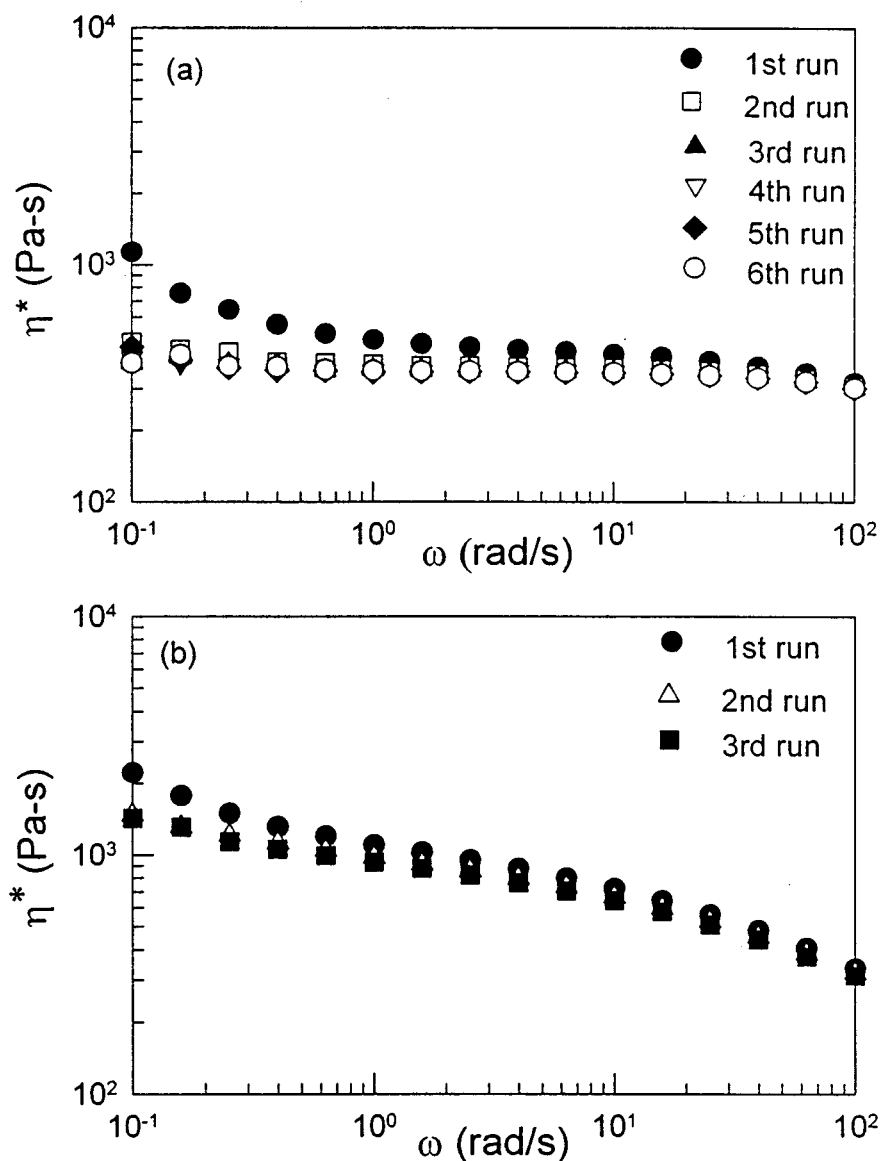


FIG. 5.  $\eta^*$  changes with repeated frequency sweeps for two different blend systems; (a) for 70/30 (wt/wt) PBT/glass fiber at 240 °C, and (b) for 60/30/10 (wt/wt/wt) PP/glass fiber/mica at 220 °C.

### B. Shear amplitude and shearing time

Figure 6 gives change in  $\eta^*(\omega)$  at  $\omega = 1$  rad/s and 220 °C with oscillatory shearing time for filled PS at four different strain amplitudes ( $\gamma_0$ ). As  $\gamma_0$  increases, the steady value of  $\eta^*(\omega)$  decreases. The maximum  $\gamma_0$  employed in this study is 30%, which falls into the linear viscoelasticity region for neat PS at 220 °C and  $\omega = 1$  rad/s. Thus, the decrease in  $\eta^*(\omega)$  with  $\gamma_0$  suggests that at higher  $\gamma_0$  more fibers in filled PS were oriented along the flow direction. It can also be seen in Fig. 6 that

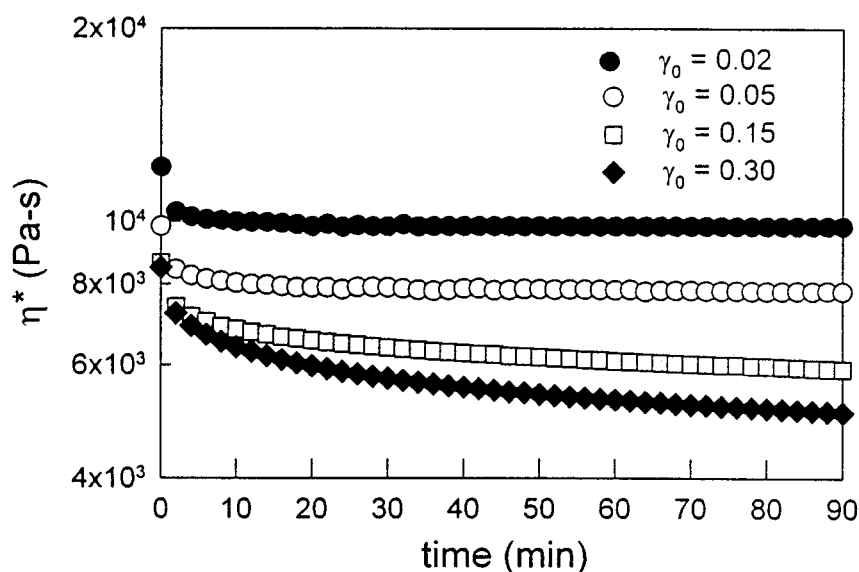


FIG. 6. Plots of  $\eta^*$  vs oscillating shearing time at  $\omega = 1.0$  rad/s and  $T = 220$  °C for 80/20 (wt/wt) PS/glass fiber as functions of strain amplitude ( $\gamma_0$ ); (●) 0.02; (○) 0.05; (□) 0.1; and (◆) 0.3.

- (i)  $\eta^*$  rapidly decreases at shorter times followed by a gradual decrease to a steady value,
- (ii)  $\eta^*(\omega, t) / \eta^*(\omega, t = \infty)$  at different  $\gamma_0$  cannot be superimposed onto a master curve even if either the cumulative strain ( $\gamma_0 t$ ) or work by strain ( $\gamma_0^2 t$ ) is used as an  $x$  axis.

Previously, Laun (1984) and Ausias *et al.* (1992) showed that when a steady shear experiment was employed for fiber-reinforced polymers,  $\eta(\dot{\gamma}, t) / \eta(\dot{\gamma}, t = \infty)$  at different shear stresses ( $\tau$ ) was superimposed onto a master curve if the  $x$  axis is taken as the total strain ( $\dot{\gamma} t$ ). Kobayashi *et al.* (1995) recently reported that the orientation of potassium titanate whiskers with a length of 10–20  $\mu\text{m}$  and diameter of 0.2–0.5  $\mu\text{m}$  in the polystyrene matrix was affected by the elongational strain and not by the elongational strain rate, even if the diameter of whiskers is much smaller than that of glass fibers employed in this study.

The results given in Fig. 6 are very similar to those found at block copolymers with lamellar microdomains [Gupta *et al.* (1995), (1996); Koppi *et al.* (1992); Riise *et al.* (1995)] or with cylindrical microdomains [Morrison and Winter (1989); Morrison *et al.* (1990)]. For instance, when an oscillatory shear with relatively larger  $\gamma_0$  is applied to a microphase separated block copolymer with lamellar microdomains oriented randomly in a macroscopic scale, lamellar microdomains can be macroscopically aligned to the shearing direction or the gradient of shearing direction depending upon the values of  $\omega$ ,  $\gamma_0$ , and temperature [Gupta *et al.* (1995), (1996)]. During the alignment of microdomains macroscopically from a random distribution the complex modulus ( $G^*$ ), thus  $\eta^*$ , shows a complex decrease with  $\gamma_0$  similar to the results shown in Fig. 6.

It can be further noticed that when an oscillatory shear with a relatively larger  $\gamma_0$  is applied to a microphase separated block copolymer with cylinders oriented randomly in macroscopic scale, the cylinder axis of the microdomain can be macroscopically aligned

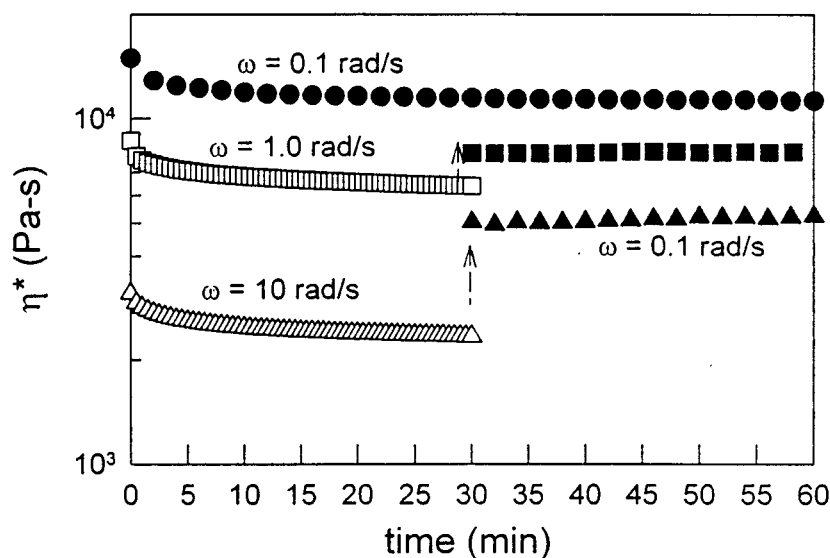


**FIG. 7.**  $\eta^*$  changes with oscillatory shearing time for 80/20 (wt/wt) PS/glass fiber at various  $\omega$  (rad/s); (●) 0.1; (□) 1.0; and (△) 10.0. Plots of  $\eta^*$  vs oscillatory shearing time at  $\omega = 0.1$  rad/s are also shown after pre-oscillatory shearing with  $\gamma_0 = 0.15$  for 30 min at two different frequencies  $\omega$  (rad/s); (■) 1.0; and (▲) 10.0. The measuring temperature was 220 °C and  $\gamma_0 = 0.15$ .

to the shearing direction [Morrison and Winter (1989); Morrison *et al.* (1990)]. In this situation,  $\eta^*(\omega)$ ,  $G'(\omega)$ , and  $G''(\omega)$  are lower than those with the cylinder axis oriented randomly in a macroscopic scale [Morrison and Winter (1989); Morrison *et al.* (1990)]. Thus, even though short glass fibers employed in this study are cylinders with the dimension much larger than the cylinder microdomains in a block copolymer, glass fibers in a viscoelastic polymer are also effectively aligned along the flow direction when an oscillatory shearing is applied.

Figure 7 gives  $\eta^*(\omega)$  changes with time measured at 220 °C and  $\gamma_0 = 0.15$  for filled PS at three different  $\omega$ . For each  $\omega$ ,  $\eta^*(\omega)$  approached a steady value at oscillatory shearing times greater than 30 min. Note that it takes about 2 min to measure each data point of  $\eta^*$  at  $\omega = 0.1$  rad/s, but this time is significantly reduced to 1.2 s to measure each data point of  $\eta^*$  at  $\omega = 10$  rad/s. It is rather interesting to find in Fig. 7 that the ratio of the initial value of  $\eta^*(\omega)$  to its steady value does not seem to vary much with  $\omega$ . However, this ratio obtained at  $\omega = 0.1$  rad/s is much smaller than that observed in Fig. 2. This is due to the fact that many frequencies are employed before measuring  $\eta^*(\omega)$  in Fig. 2, while only one frequency is used in Fig. 7. This difference can also be explained clearly when one considers the effect of pre-oscillatory shearing on  $\eta^*(\omega)$ , which is also given in Fig. 7. For instance, at  $\omega = 0.1$  rad/s the steady value of  $\eta^*$  after the pre-oscillatory shearing at  $\omega = 10$  rad/s for 30 min is  $5.0 \times 10^3$  Pa s, which is lower than that ( $8.0 \times 10^3$  Pa s) after the pre-oscillatory shearing at  $\omega = 1$  rad/s for 30 min, and much lower than that ( $1.14 \times 10^4$  Pa s) without a pre-oscillatory shearing.

Figure 8 gives the effect of the pre-oscillatory shearing time on  $\eta^*(\omega)$ . As the pre-oscillatory shearing time at  $\omega = 10$  rad/s increases, the steady values of  $\eta^*(\omega)$  measured at  $\omega = 0.1$  rad/s decrease. It can be concluded from Figs. 2 and 6–8 that when an oscillatory shearing is applied to filled polymers with glass fibers,  $\eta^*(\omega)$  and the fiber

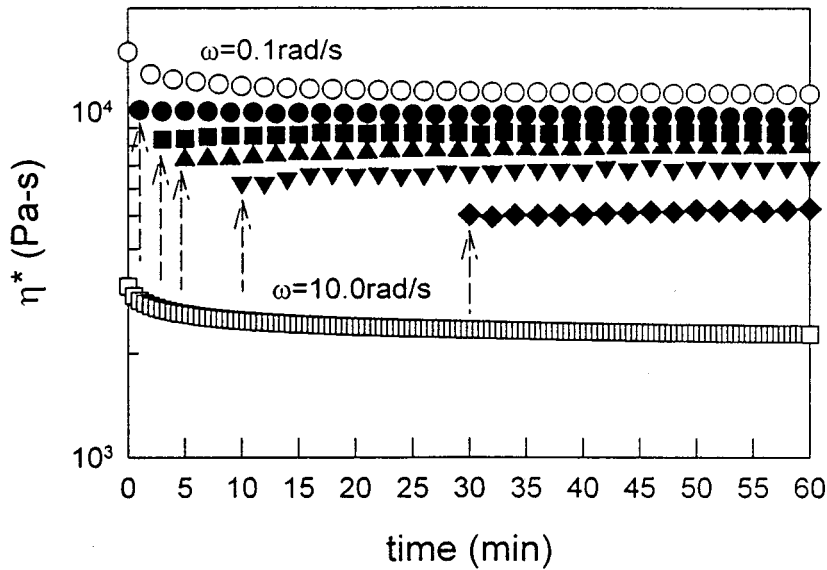


**FIG. 8.**  $\eta^*$  changes with oscillatory shearing time at  $\omega = 0.1$  rad/s for 80/20 (wt/wt) PS/glass fiber after various pre-oscillatory shearing times at  $\omega = 10$  rad/s and  $\gamma_0 = 0.15$ . Pre-shearing times (min): (●) 1; (■) 3; (▲) 5; (▼) 10; and (◆) 30. The measuring temperature was 220 °C and  $\gamma_0 = 0.15$ .

orientations show a complex variation with  $\gamma_0$ , and pre-oscillatory shearing frequency and time.

Figure 9 summarizes changes in  $\eta^*(\omega)$  at  $\omega = 0.1$  rad/s with volume fraction ( $c$ ) of glass fiber contents in filled PS. It can be noted from Fig. 9 that

- (i) as increasing  $c$ , the ratio of  $\eta^*(\omega)$  taken during the first frequency sweep to that taken during the fifth frequency sweep increased; and
- (ii) the steady value of  $\eta^*(\omega)$  at a given  $\omega$  is larger than that taken after many frequency sweeps.

### C. Fiber orientations in filled PS

Fiber orientations at three positions in filled PS prepared by compression molding, that is, before an oscillatory shearing, were observed by OM with a reflectance mode and are given in Fig. 10. Also optical microscope images at three different sample heights,  $z' = 0, 1/2$ , and 1, after five frequency sweeps are given in Figs. 11–13, respectively. Here,  $z'$  is defined by  $z/H$ , namely,  $z' = 0$  represents the sample position at the stationary plate,  $z' = 1$  represents the sample position at the oscillating plate, and  $z' = 1/2$  represents the middle height of the sample. The specimen at  $z' = 1/2$  for the OM sample was prepared by polishing the sample from the surface to this position with a paper grinder. The observing area corresponding to each position was  $\sim 4 \text{ mm}^2$ . We do not observe OM micrographs directly for specimens at  $z' = 0$  and  $z' = 1$  due to the rough surfaces. Thus, we polished the sample up to 10  $\mu\text{m}$  from each surface in order to have better OM images.

It can be seen in Fig. 10 that fibers in the sample before an oscillatory shearing are oriented randomly and do not vary with a radial position of the specimen. This is due to random orientations formed during sample preparation by compression molding. On the other hand, it can be seen in Figs. 11–13 that after many oscillatory frequency sweeps are applied, most fibers in position (c) are oriented along the flow direction, while fiber

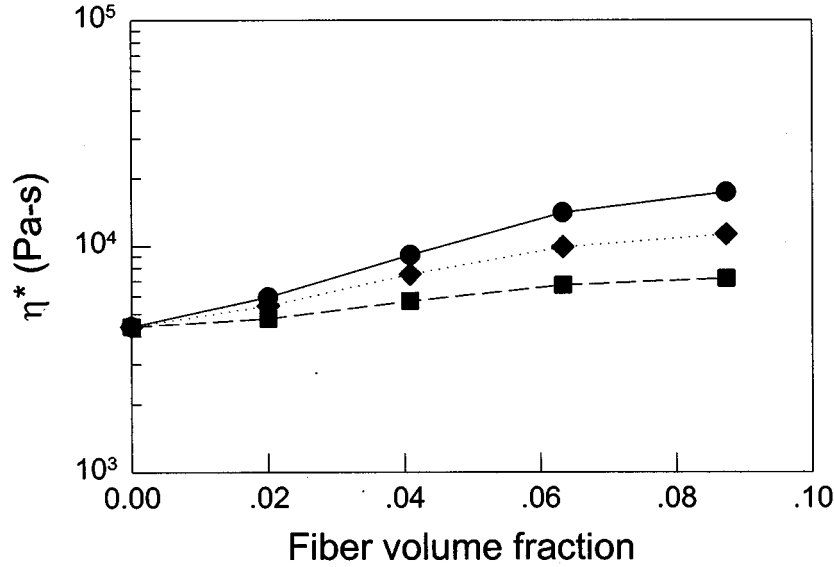


**FIG. 9.** Plots of  $\eta^*$  at  $\omega = 0.1$  rad/s vs fiber volume fraction ( $c$ ) for various sample histories; (●) without pre-oscillatory shearing; (◆) after an oscillatory shearing at  $\omega = 0.1$  rad/s and  $\gamma_0 = 0.15$  for 90 min; (■) after five frequency sweeps between 0.1 and 100 rad/s with  $\gamma_0 = 0.15$ .

orientations in position (a) are still random. This is explained by the fact that as the radial distance ( $r$ ) from the center is increased, the oscillatory shear is increased linearly, thus fibers have more chance to be aligned along the flow direction. It is of interest to note from Figs. 11–13 that fibers at position (c) become slightly less oriented along the flow direction as  $z'$  increases. This suggests that fibers at the oscillatory shearing plane are slightly less oriented along the flow direction than those at the stationary plane. This might be due to the fact that with increasing  $z'$  the centrifugal force increases. This arises from a rotation of the oscillatory shearing plane in a rheometer with a cylindrical geometry. The greater the centrifugal force, the less the fibers are aligned along the flow direction. Of course, when a rectangular geometry is employed, more fibers at the shearing plane would be aligned along the flow direction than those at the stationary plane. This will be elaborated further in the numerical simulation section.

Therefore, we conclude that an oscillatory shearing can change the fiber orientations and affects  $\eta^*(\omega)$ . This is consistent with previous experimental results (see Figs. 2, 6, and 7). However, it should be mentioned that although the qualitative determination of fiber orientations can easily be done by an optical microscopic experiment, the quantitative determination of the degree of fiber orientations at every position in the sample is rather difficult to be obtained, thus a theory to predict fiber orientations for an oscillatory shearing is needed.

#### D. Predictions of fiber orientation and viscosity

According to Folgar and Tucker (1984) and Advani and Tucker (1987), (1990), the time evolution of the fiber orientation tensors was expressed by

$$\frac{Da_{ij}}{Dt} = -\left(\frac{1}{2}\right)(\omega_{ik}a_{kj} - a_{ik}\omega_{kj}) + \left(\frac{1}{2}\right)\lambda(\dot{\gamma}_{ik}a_{kj} + a_{ik}\dot{\gamma}_{kj} - 2\dot{\gamma}_{kl}a_{ijkl}) + 2C_I\dot{\gamma}(\delta_{ij} - \alpha a_{ij}), \quad (1)$$

where  $a_{ij}$  and  $a_{ijkl}$  are the second and the fourth order orientation tensors defined by

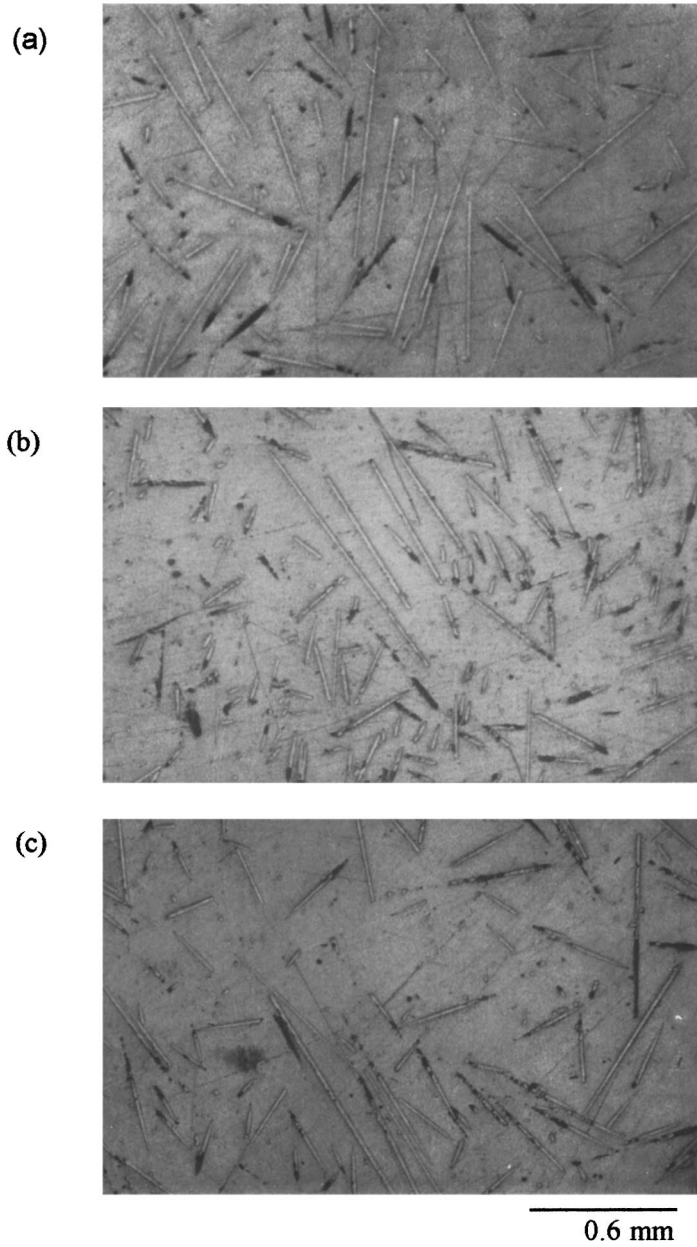


**FIG. 10.** OM photographs of fiber orientations before an oscillatory shearing at three different radial positions: (a)  $r = 0.0$ , (b)  $r = 5.0$ , (c)  $r = 10.0$  mm.

$$a_{ij} = \oint p_i p_j \psi(\mathbf{p}, t) d\mathbf{p} \quad (2)$$

$$a_{ijkl} = \oint p_i p_j p_k p_l \psi(\mathbf{p}, t) d\mathbf{p},$$

in which  $\psi(\mathbf{p}, t)$  is the probability distribution function of a fiber having an alignment in the direction of director  $\mathbf{p}$ .  $\omega_{ij}$  and  $\dot{\gamma}_{ij}$  in Eq. (1) are the vorticity and the rate of

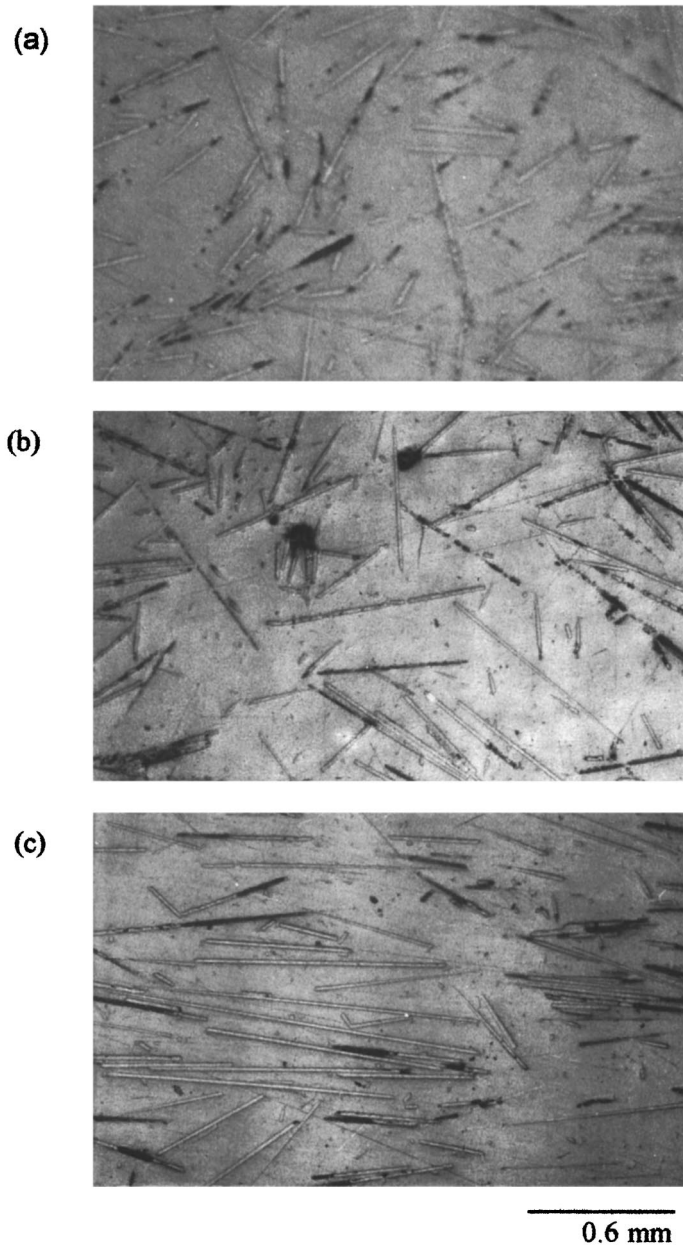


**FIG. 11.** OM photographs of fiber orientations at  $z' = 0$  (i.e., the stationary plane) after five frequency sweeps between 0.1 and 100 rad/s with  $\gamma_0 = 0.15$  at three different radial positions: (a)  $r = 0.0$ , (b)  $r = 5.0$ , (c)  $r = 10.0$  mm.

deformation tensors, respectively,  $\delta_{ij}$  is the unit tensor,  $\dot{\gamma}$  is the second invariant of the rate of deformation tensor,  $\alpha$  is equal to three for three-dimensional analysis, and  $\lambda$  is a fiber shape factor defined by

$$\lambda = \frac{r_e^2 - 1}{r_e^2 + 1}, \quad (3)$$

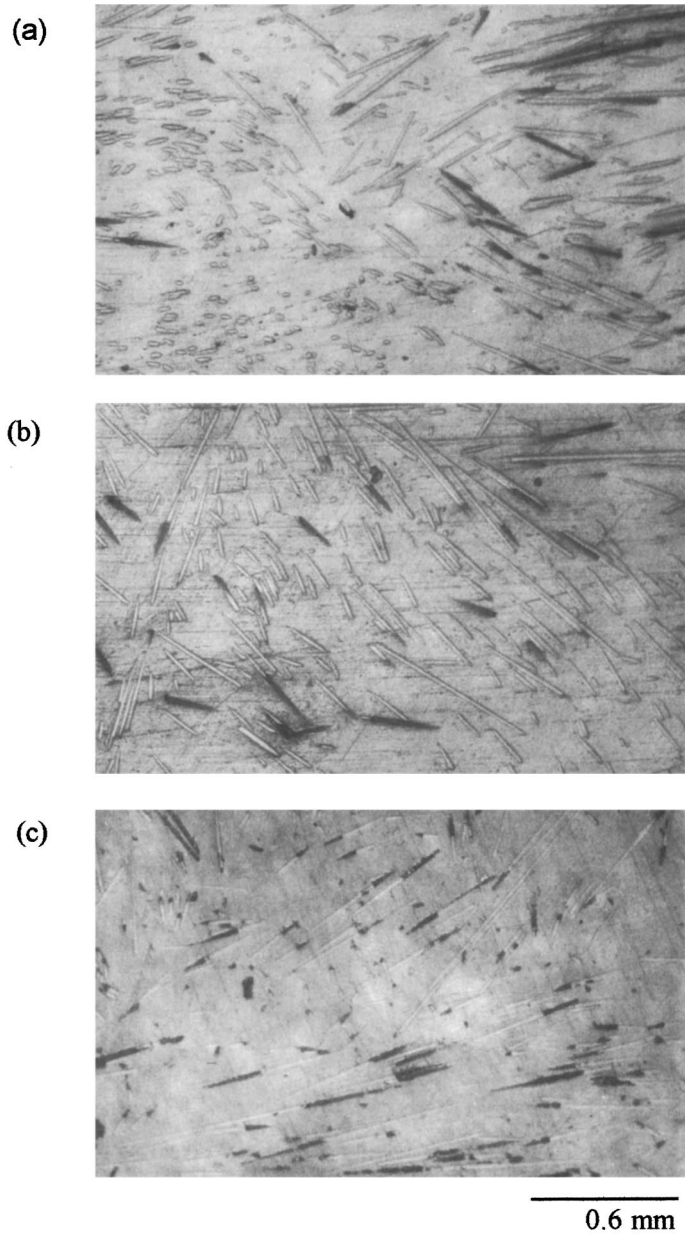


**FIG. 12.** OM photographs of fiber orientations at  $z' = 0.5$  after five frequency sweeps between 0.1 and 100 rad/s with  $\gamma_0 = 0.15$  at three different radial positions: (a)  $r = 0.0$ , (b)  $r = 5.0$ , (c)  $r = 10.0$  mm.

in which  $r_e$  is the aspect ratio of the fiber (i.e.,  $L/D$ , where  $L$  and  $D$  are the length and the diameter of the fiber). Although  $C_I$  in Eq. (1) is related to the critical distance from a test fiber to its nearest neighbors, it can be considered as a phenomenological parameter depending upon the aspect ratio of the fiber, orientation of the fiber, and fiber volume fraction [Tucker and Advani (1994)]. According to Tucker and Advani (1994),  $C_I$  increases with the product of the volume fraction ( $c$ ) and the aspect ratio ( $L/D$ ) of fiber

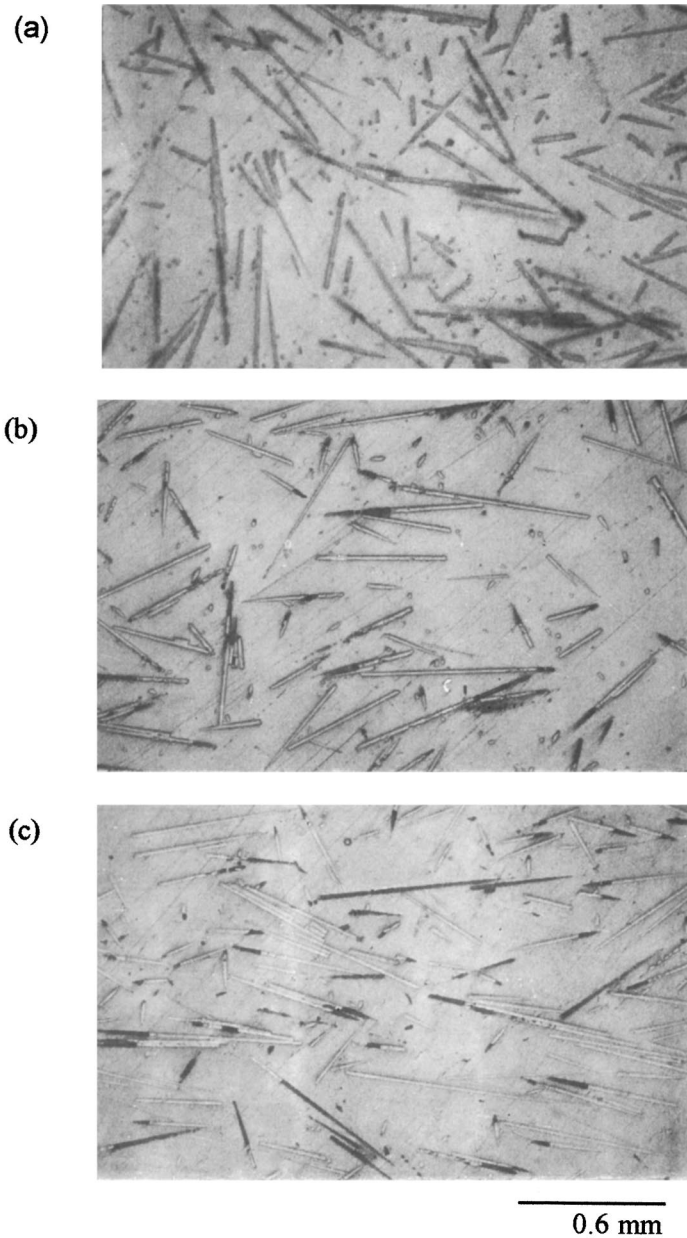


**FIG. 13.** OM photographs of fiber orientations at  $z' = 1$  (the shearing plane) after five frequency sweeps between 0.1 and 100 rad/s with  $\gamma_0 = 0.15$  at three different radial positions: (a)  $r = 0.0$ , (b)  $r = 5.0$ , (c)  $r = 10.0$  mm.

when  $c(L/D)$  is less than 1 (i.e., dilute and semi-dilute regimes), but  $C_I$  decreases with increasing  $c(L/D)$  for  $c(L/D) > 1$  (i.e., concentrated regimes) as follows:

$$C_1 = 0.0184 \exp[-0.7148c(L/D)]. \quad (4)$$

For oscillatory shear strain with parallel plate geometry [ $(r, \theta, z)$  coordinate]  $\dot{\gamma}_{ij}$  and  $\omega_{ij}$  in Eq. (1) are given by

$$\dot{\gamma} = \begin{vmatrix} 0 & 0 & 0 \\ 0 & 0 & \omega r \gamma_0 \cos(\omega t)/H \\ 0 & \omega r \gamma_0 \cos(\omega t)/H & 0 \end{vmatrix}, \quad (5a)$$

$$\omega = \begin{vmatrix} 0 & 2\omega z \gamma_0 \cos(\omega t)/H & 0 \\ -2\omega z \gamma_0 \cos(\omega t)/H & 0 & -\omega r \gamma_0 \cos(\omega t)/H \\ 0 & \omega r \gamma_0 \cos(\omega t)/H & 0 \end{vmatrix}, \quad (5b)$$

where  $\omega$  is the angular frequency (rad/s),  $r$  is the radial position from the center,  $\gamma_0$  is the strain amplitude,  $t$  is the oscillatory shearing time,  $z$  is the height from the stationary plate, and  $H$  is the gap between parallel plates. In calculation of the fourth order tensor,  $a_{ijkl}$ , we use the following decoupling technique advocated by Advani and Tucker (1990)

$$a_{ijkl} = (1-f)\hat{a}_{ijkl} + f\tilde{a}_{ijkl}, \quad (6)$$

where  $\hat{a}_{ijkl}$  and  $\tilde{a}_{ijkl}$  are the linear and quadratic closure approximation, respectively, and defined by

$$\hat{a}_{ijkl} = \{a_{ij}\delta_{kl} + a_{kl}\delta_{ij} + a_{ik}\delta_{jl} + a_{jl}\delta_{ik} + a_{jk}\delta_{il} + a_{il}\delta_{jk}\}/7 - \{\delta_{ij}\delta_{kl} + \delta_{ik}\delta_{jl} + \delta_{il}\delta_{jk}\}/35, \quad (7a)$$

$$\tilde{a}_{ijkl} = a_{ij}a_{kl}. \quad (7b)$$

Also,  $f$  represents the degree of the orientations and is given by [Advani and Tucker (1990)]

$$f = 1 - 27 \det[a_{ij}]. \quad (8)$$

Figure 14 gives the steady values of  $f$  at various radial and height positions, which were obtained by substituting Eq. (5) into Eq. (1) with the aid of Eqs. (6)–(8). Because of the use of Eq. (5), each component in the orientation tensors can still oscillate with time, and even at longer times. However, since the variation in this value with time becomes smaller at longer shearing times, one can have the average value of  $f$  given in Fig. 14 by just averaging  $f$  taken for a certain interval at longer times. In this numerical calculation, the Runge–Kutta fourth order numerical method was employed to integrate Eq. (1). It should be noted that even if other decoupling techniques such as the Hinch–Leal method (1973) are employed,  $f$  behaves very similarly to that obtained by a hybrid method employed in this study although numerical values are slightly changed. In this study,  $C_I$  was obtained according to Eq. (4), for instance, when  $c = 0.0874$  (i.e., weight fraction of fibers = 0.2) and  $L/D = 54$ ,  $C_I$  was calculated to be  $5.97 \times 10^{-4}$ . We found that the difference between the orientation tensor component  $a_{ij}$  obtained with  $C_I = 5.97 \times 10^{-4}$  and that with  $C_I = 0.01$  is rather small, although the value obtained with  $C_I = 0$  is rather different from that obtained with  $C_I = 5.97 \times 10^{-4}$ . Thus, any uncertainty incurred in estimating the  $C_I$  value employed in this calculation affects little, if any, the prediction of fiber orientations.

It can be seen in Fig. 14 that  $f$  increases steadily with increasing radial position, which is well consistent with experimental results given in Figs. 11–13. On the other hand, at larger  $r$  (say  $r/R > 0.6$ ),  $f$  becomes smaller with increasing  $z$ . The reason is that as  $z$  increases (i.e., closer to rotating plate) the absolute values of  $\omega_{12}$  and  $\omega_{21}$  terms in the vorticity tensor given in Eq. (5) becomes larger, thus  $f$  becomes smaller. This means that

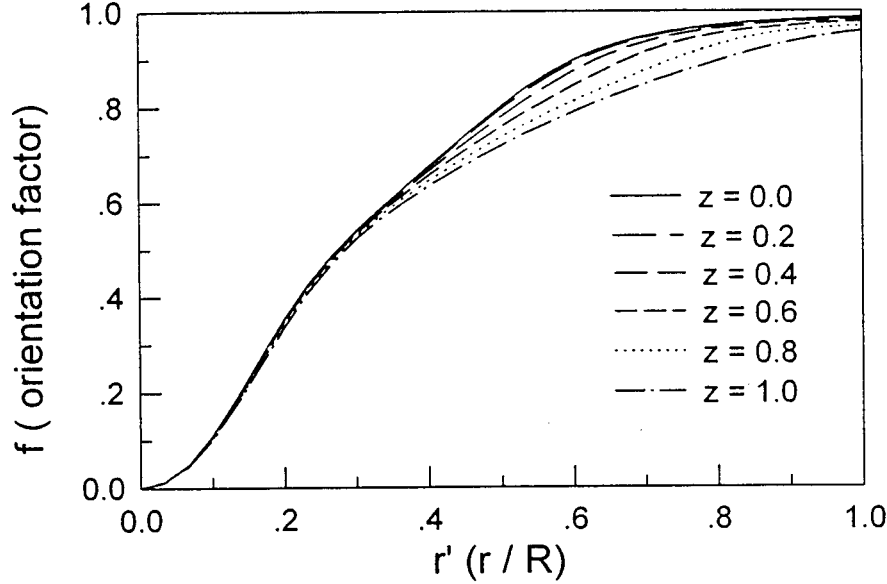


FIG. 14. Predicted values of the fiber orientation factor ( $f$ ) at various radial ( $r$ ) and height ( $z'$ ) positions, where  $\gamma_0 = 1.0$  and  $C_I = 5.97 \times 10^{-4}$  are used.

the rotation prevents fibers from being oriented along the flow direction due to the centrifugal force. This is also consistent with experimental results given in Figs. 11–13.

Figure 15 shows that as  $\gamma_0$  increases, the fiber orientation along the flow direction increases, thus  $\eta^*(\omega)$  decreases, which is consistent with experimental results shown in Fig. 6. However, the above predictions cannot explain the fiber orientation change with the magnitude of frequency and shear history since predicted fiber orientations are independent of frequency at longer shearing times.

Once fiber orientations are calculated, the viscosity can be estimated by the following constitutive equations [Dinh and Armstrong (DA) (1984)]

$$\tau_{ij} = \eta_m(\dot{\gamma}_{ij} + Aca_{ijkl}\dot{\gamma}_{ij}), \quad (9)$$

where  $\tau_{ij}$  is the total stress tensor,  $\eta_m$  is the viscosity of matrix polymer, and  $c$  is the volume fraction of fiber. The parameter  $A$  is defined by [Dinh and Armstrong (1984)]

$$A = \frac{(L/D)^2}{3 \ln(2h/D)}, \quad (10)$$

where  $h$  is the average distance from a test fiber to its nearest neighbors

$$h = \begin{cases} (1-f)\pi D/(4cr_e) + fD(\pi/c)^{1/2}/2 & \text{for } (1/r_e^2) < c < 1/r_e \\ D(\pi/c)^{1/2}/2 & \text{for } 1/r_e \leq c \end{cases}. \quad (11)$$

Ranganathan and Advani (RA) (1991) obtained  $h$  in Eq. (10) by modifying Doi and Edwards (1978) theory for rigid rodlike molecules as follows:

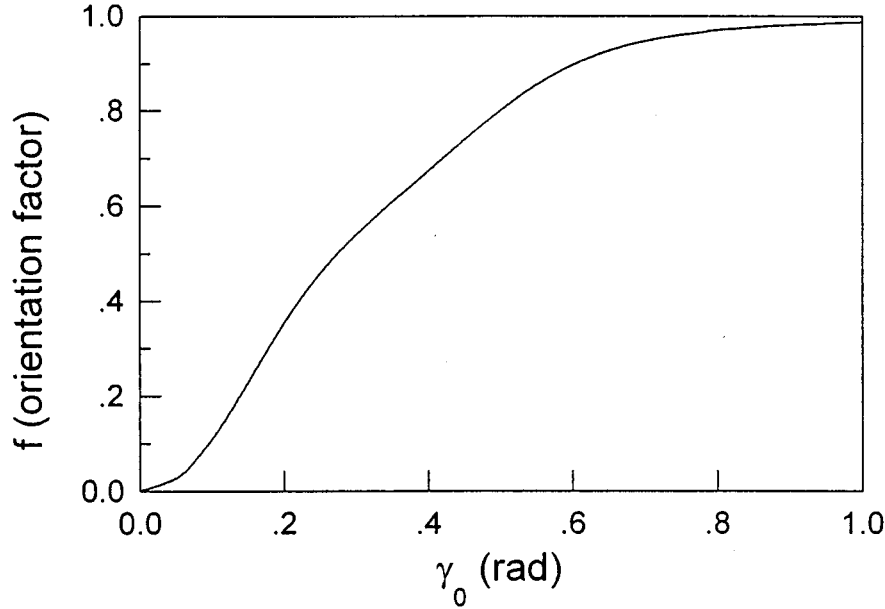


FIG. 15. Predicted values of the fiber orientation factor ( $f$ ) as functions of  $\gamma_0$  at  $r = 12.5$  mm and  $z' = 0.0$ .

$$h = \begin{cases} \frac{-1 + [1 + 6/(cr_e^2)]^{1/2}}{(6/L)} & \text{for random orientation} \\ D/(8c)^{1/2} & \text{for full alignment} \end{cases} \quad (12)$$

Since all  $a_{ijkl}$  at every position inside the parallel plates can be calculated, one can obtain viscosity at that position, thus the average relative complex viscosity ( $\eta_r^*$ ) of filled PS can be calculated:

$$\eta_r^* = \frac{2 \int_0^H \int_0^R \eta_r^*(r,z) r dr dz}{R^2 H}, \quad (13)$$

where the relative complex viscosity  $\eta_r^*(r,z)$  at each position is given by

$$\eta_r^*(r,z) = \frac{\eta^*(r,z)}{\eta_m} = 1 + Ac(a_{2323} + a_{2332}). \quad (14)$$

Numerical integration of Eq. (13) was done by the composite Simpson rule using ten intervals for both  $r$  and  $z$ . It should be mentioned that because of using Eq. (5),  $a_{2332}$ , thus  $\eta_r^*$  in Eq. (14) can still oscillate with time. However, one can have the average value of  $\eta_r^*$  at each time by averaging this taken for a short interval around that time. We found that as shearing time increases, the predicted value of  $\eta_r^*/\eta_{r,0}^*$  decreases, and then reaches a steady value at longer times, where  $\eta_{r,0}^*$  is the initial value of  $\eta_r^*$ , that is, the relative viscosity at a random orientation.

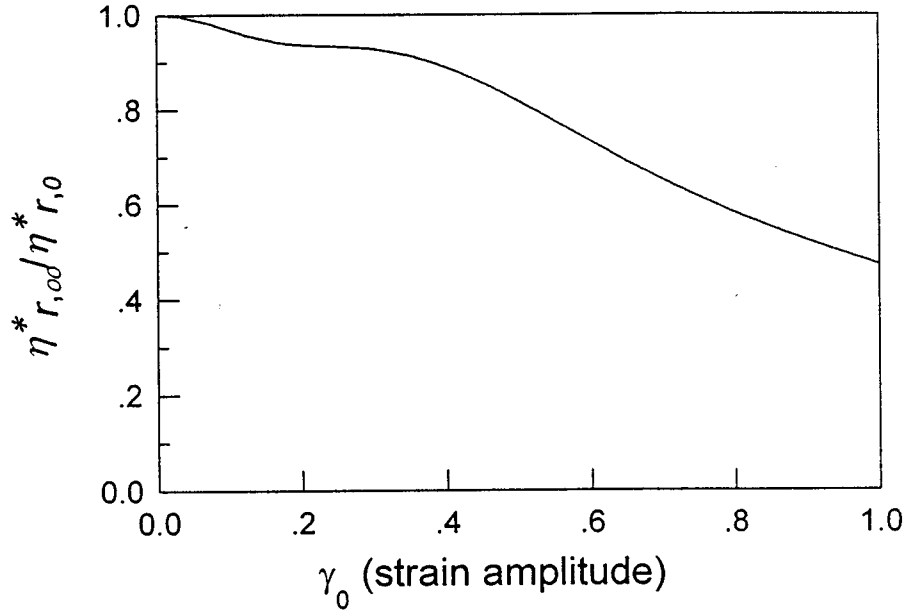


FIG. 16. Change in predicted value of  $\eta_{r,\infty}^*/\eta_{r,0}^*$  with  $\gamma_0$  for  $c = 0.0874$  and  $\omega = 0.1$  rad/s.

The predicted values of  $\eta_{r,\infty}^*/\eta_{r,0}^*$  at various  $\gamma_0$  are given in Fig. 16, where  $\eta_{r,\infty}^*$  is the relative viscosity taken at longer times ( $t > 60$ ). It can be seen that the higher  $\gamma_0$  is, the larger the reduction in relative viscosity. This is because more fibers are aligned along the flow direction. The results given in Fig. 16 are in a qualitative agreement with experimental results given in Fig. 6. However, it should be mentioned that the numerical predictions give the same  $\eta_{r,\infty}^*$  regardless of  $\omega$  at longer times ( $t > 20$ ).

Figure 17 gives a comparison of predicted values of  $\eta_{r,\infty}^*/\eta_{r,0}^*$  with experimental data for filled PS given in Fig. 9. It has been found that the predicted values of  $\eta_{r,\infty}^*/\eta_{r,0}^*$  by RA theory [i.e., Eq. (12)] are almost the same as those predicted by the DA theory [i.e., Eq. (11)]. It can be seen in Fig. 17 that although predicted values of  $\eta_{r,\infty}^*/\eta_{r,0}^*$  are in qualitative agreement with experimental data, that is they decrease with increasing  $c$ , a theory which gives better agreement between prediction and experimental data is needed.

Recently, Shaqfeh and Fredrickson (SF) (1990) developed a theory which enables one to predict the relative viscosity ( $\eta_r$ ) for semi-diluted filled polymer system with two different fiber orientations. For random orientation of fibers, the parameter  $A$  in Eq. (9) is given by

$$A_{\text{random}} = \frac{16(L/D)^2}{3 \ln(1/c)} \left[ 1 - \frac{\ln[\ln(1/c)]}{\ln(1/c)} + \frac{0.6634}{\ln(1/c)} \right], \quad (15a)$$

while for perfect aligned orientation of fibers, the parameter  $A$  is given by

$$A_{\text{align}} = \frac{16(L/D)^2}{3\{\ln(1/c) + \ln[\ln(1/c)] + 0.1585\}}. \quad (15b)$$

In this numerical calculation, we assume that  $A$  in Eq. (14) can be given by

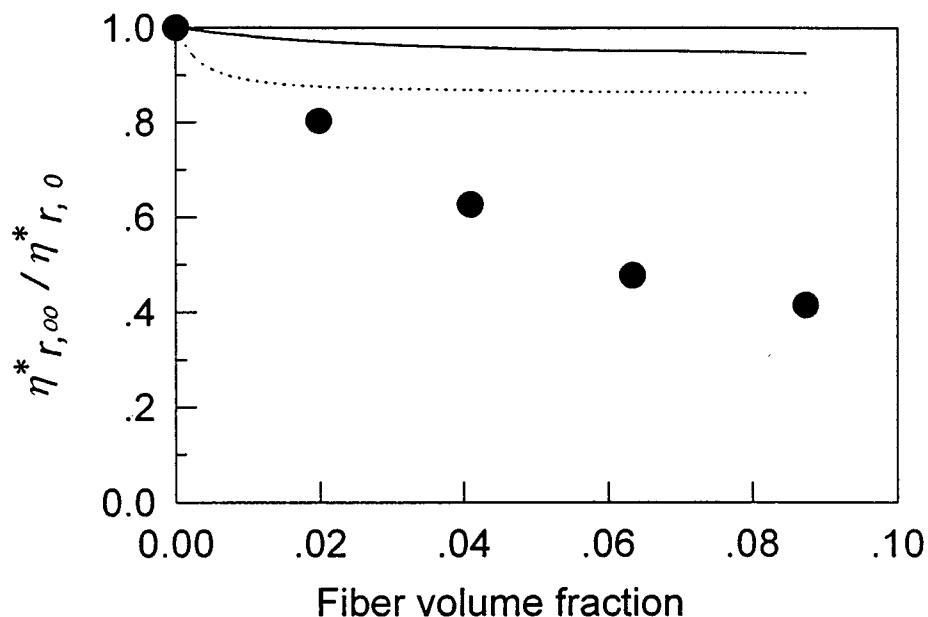


FIG. 17. Prediction by DA [(—) and by SF (---)], and experimental data (●) of  $\eta_{r,\infty}^*/\eta_{r,0}^*$  at  $\omega = 0.1$  rad/s and  $\gamma_0 = 0.15$  as functions of fiber volume fraction.

$$A = (1 - \bar{f})A_{\text{random}} + \bar{f}A_{\text{align}}, \quad (16)$$

where  $\bar{f}$  is the average value of  $f$  obtained by the numerical integration of Eq. (13) with substitution of  $\eta_r^*(r,z)$  to  $f(r,z)$ . Predicted values of  $\eta_{r,\infty}^*/\eta_{r,0}^*$  by the SF theory at various values of  $c$  are also given in Fig. 17, from which SF theory gives slightly better results than the DA theory. However, it is recommended that a rigorous theory giving better agreement between prediction and experimental data be developed.

#### IV. CONCLUDING REMARKS

In this study, we have shown that the rheological properties of the short glass fiber-reinforced composites are strongly affected by the fiber orientations, especially for higher fiber volume fractions. As the fibers in suspension are effectively aligned to the flow direction from the initial random orientation by an oscillatory shear,  $\eta^*$  gradually decreases. This phenomenon was confirmed by observing the fiber orientations using OM photographs.

The yield behavior was found for fiber filled polymers during the first frequency sweep. However, this yield behavior can barely be seen after five frequency sweeps. This is attributed to the fact that the fiber orientations reached a steady state. The complex viscosity as well as fiber orientation for the fiber filled polymers depends not only on  $\gamma_0$  but pre-oscillatory shearing frequency and time. These results are very similar to those found at block copolymers with the lamellar microdomain structure studied by Gupta *et al.* (1995), (1996) who showed that the alignment of lamellar layers to the shearing flow direction or to the gradient of shearing direction varied very complicatedly with  $\omega$ ,

$\gamma_0$ , and pre-oscillatory shearing time and frequency. In other words, fiber orientations during oscillatory flow are more complex than predicted by many theories [Advani and Tucker (1987), (1990); Tucker and Advani (1994)] available at the present time.

Experimental results for  $\eta^*$  or fiber orientations were compared with predictions available at the present time. Predictions of the fiber orientation depending upon the strain amplitude and the fiber volume fraction are in qualitative agreement with experimental data. However, the effects of the frequency and pre-oscillatory shearing time on the fiber orientation, thus  $\eta^*$ , cannot be predicted successfully although these effects are clearly demonstrated by the experiment.

## ACKNOWLEDGMENT

The authors thank H. K. Jeon for assisting in the steady shear measurement of filled PS. This work was supported by NON DIRECTED RESEARCH FUND (1996), Korea Research Foundation, Korea, and in part by the Korean Science and Engineering Foundation through the Automation Research Center at Pohang University of Science and Technology, Korea.

## References

- Advani, S. G. and C. L. Tucker, III, "The use of tensors to describe and predict fiber orientation in short fiber composites," *J. Rheol.* **31**, 751–784 (1987).
- Advani, S. G. and C. L. Tucker III, "Closure approximations for three-dimensional structure tensors," *J. Rheol.* **34**, 367–386 (1990).
- Ausias, G., J. F. Agassant, M. Vincent, P. G. Lafleur, P. A. Lavoie, and P. J. Carreau, "Rheology of short glass fiber reinforced polypropylene," *J. Rheol.* **36**, 525–542 (1992).
- Batchelor, G. K., "Stress generated in a non-dilute suspension of elongated particles by pure straining motion," *J. Fluid Mech.* **46**, 813–829 (1971).
- Becraft, M. L. and A. B. Metzger, "The rheology, fiber orientation, and processing behavior of fiber-filled fluids," *J. Rheol.* **36**, 143–174 (1992).
- Creasy, T. S., S. G. Advani, and R. K. Okine, "Transient rheological behavior of a long discontinuous fiber-melt system," *J. Rheol.* **40**, 497–519 (1996).
- Czarniecki, L. and J. L. White, "Shear flow rheological properties, fiber damage, and mastication characteristics of aramid-, glass-, and cellulose-fiber reinforced polystyrene melts," *J. Appl. Polym. Sci.* **25**, 1217–1244 (1980).
- Dinh, S. M. and R. C. Armstrong, "A rheological equation of state for semi-concentrated fiber suspensions," *J. Rheol.* **28**, 207–227 (1984).
- Doi, M. and S. F. Edwards, "Dynamics of rod-like macromolecules in concentrated solution," *J. Chem. Soc. Faraday Trans. 2* **74**, 560–570 (1978).
- Folgar, F. and C. L. Tucker, "Orientation behavior of fibers in concentrated suspensions," *J. Reinf. Plast. Compos.* **3**, 98–119 (1984).
- Greene, J. P. and J. O. Wilkes, "Steady-state and dynamic properties of concentrated fiber-filled thermoplastics," *Polym. Eng. Sci.* **35**, 1670–1681 (1995).
- Gupta, V. K., R. Krishnamoorti, J. A. Kornfield, and S. D. Smith, "Evolution of microstructure during shear alignment in a polystyrene-polyisoprene lamellar diblock copolymer," *Macromolecules* **28**, 4464–4474 (1995).
- Gupta, V. K., R. Krishnamoorti, Z. R. Chen, J. A. Kornfield, S. D. Smith, M. M. Sathowski, and J. T. Grothaus, "Dynamics of shear alignment in a lamellar diblock copolymer: Interplay of frequency, strain amplitude, and temperature," *Macromolecules* **29**, 875–884 (1996).
- Han, C. D., *Multiphase Flow in Polymer Processing* (Academic, New York, 1981), pp. 81–147.
- Han, C. D. and J. K. Kim, "Molecular theory for the viscoelasticity of compatible polymer mixtures. 2. Tube model with reptation and constraint release contributions," *Macromolecules* **22**, 4292–4302 (1989).
- Han, C. D. and J. K. Kim, "On the use of the time-temperature superposition in multiphase and multicomponent polymer systems," *Polymer* **34**, 2533–2539 (1993).
- Hand, G. L., "A theory of anisotropic fluids," *J. Fluid Mech.* **13**, 33–46 (1962).
- Hinch, E. J. and L. G. Leal, "Time-dependent shear flows of a suspension of particles with weak Brownian rotations," *J. Fluid Mech.* **57**, 753–767 (1973).
- Jeffery, G. B. "The motion of ellipsoidal particles immersed in a viscous fluid," *Proc. R. Soc. London Ser., A* **102**, 161–179 (1922).

- Kobayashi, M., T. Takahashi, J. Takimoto, and K. Koyama, "Flow-induced whisker orientation and viscosity for molten composite systems in a uniaxial elongational flow field," *Polymer* **36**, 3927–3933 (1995).
- Koppi, K. A., M. Tirrel, F. S. Bates, K. Almdal, and R. H. Colby, "Lamellar orientation in dynamically sheared diblock copolymer melts," *J. Phys. (France) II* **2**, 1941–1959 (1992).
- Laun, H. M., "Orientation effects and rheology of short glass fiber-reinforced thermoplastics," *Colloid Polym. Sci.* **262**, 257–269 (1984).
- Lipscomb, G. G., M. M. Denn, D. U. Hur, and D. V. Boger, "The flow of fiber suspensions in complex geometries," *J. Non-Newtonian Fluid Mech.* **26**, 297–325 (1988).
- Lobe, V. M. and J. L. White, "An experimental study of the influence of carbon black on the rheological properties of a polystyrene melts," *Polym. Eng. Sci.* **19**, 617–624 (1979).
- Milliken, W. J. and R. L. Powell, "Short fiber suspensions," in *Flow and Rheology in Polymer Composites Manufacturing*, edited by S. G. Advani (Elsevier, New York, 1994), pp. 53–84.
- Morrison, F. A. and H. H. Winter, "Effect of unidirectional shear on the structure of triblock copolymers. 1. Polystyrene-polybutadiene-Polystyrene," *Macromolecules* **22**, 3533–3540 (1989).
- Morrison, F. A., H. H. Winter, W. Gronski, and J. D. Barnes, "Effect of unidirectional shear on the structure of triblock copolymers. 2. Polystyrene-polyisoprene-Polystyrene," *Macromolecules* **23**, 4200–4205 (1990).
- Ranganathan, R. and S. G. Advani, "Fiber-fiber interactions in homogeneous flows of nondilute suspensions," *J. Rheol.* **35**, 1499–1522 (1991).
- Ranganathan, S. and S. G. Advani, "A simultaneous solution for flow and fiber orientation in axisymmetric diverging radial flow," *J. Non-Newtonian Fluid Mech.* **47**, 107–136 (1993).
- Riise, B. L., G. H. Fredrickson, R. G. Larson, and D. S. Pearson, "Rheology and shear-induced alignment of lamellar diblock and triblock copolymers," *Macromolecules* **28**, 7653–7659 (1995).
- Shaqfeh, S. G. and G. H. Fredrickson, "The hydrodynamic stress in a suspension of rods," *Phys. Fluids* **2**, 7–24 (1990).
- Tanaka, H. and J. L. White, "Experimental investigation of shear and elongational flow properties of polystyrene melts reinforced with calcium carbonate, titanium dioxide, and carbon black," *Polym. Eng. Sci.* **20**, 949–956 (1980).
- Tucker, III, C. L. and S. G. Advani, "Processing of short-fiber systems," in *Flow and Rheology in Polymer Composites Manufacturing*, edited by S. G. Advani (Elsevier, New York, 1994), pp. 147–202.
- Wang, S. Q. and Y. W. Inn, "Stress-induced interfacial failure in filled polymer melts," *Rheol. Acta* **33**, 108–116 (1994).
- White, J. L., *Principles of Polymer Engineering Rheology* (Wiley, New York, 1990), pp. 160–167.